JOURNAL OF MATERIALS SCIENCE 29 (1994) 3384–3392

Solid-state synthesis and characterization of the ternary phase Ti_3SiC_2

C. RACAULT, F. LANGLAIS, R. NASLAIN
Laboratoire des Composites Thermostructuraux (UMR-47 CNRS-SEP-UB1), Domaine Universitaire, 3 allée de La Boëtie, 33600 Pessac, France

Ti_3SiC_2 is the only true ternary compound in the Ti–Si–C system. It seems to exhibit promising thermal and mechanical behaviour. With the exception of its layered crystal structure, most of its properties are unknown, owing to the great difficulty of synthesis. A new procedure of solid-state synthesis with several steps is proposed, which results in Ti_3SiC_2 with less than 5 at% of TiC. Ti_3SiC_2 is stable at least up to 1300 °C. Beyond this temperature, it can decompose with formation of non-stoichiometric titanium carbide and gaseous silicon, with kinetics highly dependent on the nature of the surroundings. As an example, graphite can initiate this process by reacting with silicon, while alumina does not favour the decomposition which remains very slow. The oxidation of Ti_3SiC_2 under flowing oxygen starts at 400 °C with formation of anatase-type TiO_2 film, as studied by TGA, XRD, SEM and AES. Between 650 and 850 °C both rutile and anatase are formed, rapidly becoming protecting films and giving rise to slow formation of SiO_2 and more TiO_2. The oxidation kinetics is slower than for TiC, owing to a protecting effect of silica. By increasing the temperature, both oxidation processes (i.e. direct reaction and diffusion through oxide layers) are activated and an almost total oxidation is achieved between 1050 and 1250 °C resulting in titania (rutile) and silica (cristobalite).

1. Introduction

In the Ti–Si–C system, Ti_3SiC_2 is known to be the only true ternary compound. Its crystal structure was determined 25 years ago by Jeitschko and Novotny [1]. Recently, Ti_3SiC_2 was identified at the SiC–Ti interface, frequently studied for the joining of ceramics and metals [2–9]. To our knowledge this compound has been prepared as a pure phase only three times. The first synthesis, by Jeitschko and Novotny, was in the solid state via a chemical reaction between TiH_2, silicon and graphite at 2000 °C [1]. The two others were from the vapour phase, using $SiCl_4$, $TiCl_4$, CCl_4 and H_2 as precursor species [10, 11]. All the authors pointed out the very limited range of experimental conditions favourable to obtaining Ti_3SiC_2 as a pure phase. Nickl *et al.* [10] prepared Ti_3SiC_2 deposits containing a small amount of $TiSi_2$ removed by an HF-based treatment [10]. A recent attempt to prepare the ternary phase by using powders of Ti, Si and carbon black was carried by Pampuch *et al.* [12], but small amounts of TiC were always formed with Ti_3SiC_2.

Owing to preparation difficulties, little is known on the properties of Ti_3SiC_2. Its crystal structure was reported to be hexagonal with the space group $P6_3/mmc$. Ti_3SiC_2 can be described as a layered compound consisting of Ti_3C_2 blocks of octahedrally coordinated carbons stacked in the *c* direction and separated by a layer of silicon atoms [1]. The density of Ti_3SiC_2 prepared by chemical vapour deposition (CVD) is 4.53 $g\,cm^{-3}$, a value slightly lower than that of stoichiometric TiC (4.70) [11].

The mechanical properties of Ti_3SiC_2 have been scarcely studied (mainly on the basis of hardness measurements) and the results are not in accordance: a plastic behaviour was reported for the phase prepared by CVD, but was not found if Ti_3SiC_2 was obtained by solid-state diffusion [10, 11]. The Knoop hardness measurements by Nickl *et al.* [10] on small Ti_3SiC_2 single crystals indicated a high anisotropy, which is in agreement with the layered crystal structure. Finally, thermodynamic data for the formation of Ti_3SiC_2 (i.e. the free energy ΔG_f°) were derived very recently from (i) measurements of the mole fraction of carbon in TiC_x in equilibrium with SiC and Ti_3SiC_2, and (ii) thermodynamic models previously used for TiC_x [13]. Up to now, no data were reported to our knowledge about important properties of Ti_3SiC_2 such as thermal stability and oxidation resistance.

In the present study, a procedure of solid-state synthesis is proposed which can advantageously replace the very difficult one-step synthesis reported by Jeitschko and Novotny [1]. After a determination of the purity of the resulting ternary phase Ti_3SiC_2, its behaviour under vacuum, inert gas and oxygen was investigated and the thermal stability and oxidation resistance deduced. Thermal expansion was also determined.

0022–2461

2. Results and discussion

2.1 Ti_3SiC_2 synthesis

Many attempts were made to prepare in a single step the ternary compound Ti_3SiC_2 according to a solid-state approach. Various mixtures were used: stoichiometric or non-stoichiometric compositions of Ti, Si and C elements or binary phases such as $TiSi_2$, Ti_5Si_3, TiC and SiC. Various experimental conditions were also tried, in terms of temperature, pressure, environment and time. In all cases, mixtures of several phases were found, TiC and silicides such as $TiSi_2$ and Ti_5Si_3 occurring very often besides Ti_3SiC_2. The presently chosen route to the ternary phase is not direct.

The first step is the reaction of a mixture of titanium powder (99.9%, Johnson Matthey), silicon powder (> 99%, Merck), and graphite powder (> 99.5%, Merck) with the respective molar fractions 0.42, 0.29 and 0.29. A pellet is prepared with this homogeneous mixture and put in an evacuated silica tube. A 10 h treatment at 1100 °C leads to a mixture of Ti_3SiC_2, $TiSi_2$ and TiC, as shown by X-ray diffraction (XRD) analysis.

The second step of the procedure is to remove $TiSi_2$ by aqueous hydrogen fluoride leading according to the equation

$$TiSi_2 + 12(HF)_{aq} \rightarrow (TiF_4)_{aq} + 2SiF_4 + 6H_2 \quad (1)$$

Silicon is removed by SiF_4 evolution and titanium by dissolving TiF_4 in water. After neutralizing the HF excess by ammonia, rinsing in water and drying, the resulting two-phase mixture contains about 85% Ti_3SiC_2 and 15% TiC, according to XRD and electron probe microanalysis (EPMA) analyses.

To remove TiC from the mixture, the fact that TiC has oxidation kinetics higher than Ti_3SiC_2 (as shown in section 2.3 below) is used in the third step. A controlled oxidation at 450 °C in air for about 10 h turns the previous mixture into a Ti_3SiC_2–TiO_2 mixture. Several successive treatments of this type with grinding are needed to oxidize the majority of the titanium carbide.

The last step is dissolving TiO_2 at about 100 °C in $(NH_4)_2SO_4$ and aqueous H_2SO_4. The titanium sulphate is dissolved in H_2SO_4 and ammonia in water. After neutralizing by NH_3, filtration and drying, the solid residue is analysed and characterized.

The XRD pattern of the solid clearly exhibits the peaks of Ti_3SiC_2 phase (Fig. 1). No extra line occurs except a very small one (d = 0.1302 nm), which probably corresponds to titanium carbide occurring as impurity. This result was confirmed by a chemical analysis performed at Laboratoire Central d'Analyse du CNRS (Vernaison); the carbon amount was obtained by infrared detection of CO_2 formed from solid burning, while the titanium and silicon amounts were determined by plasma emission spectroscopy after melting with lithium tetraborate. The atomic composition of the solid (at %) was found to be 50.4 Ti, 16.0 Si and 33.6 C (with respect to: 50 Ti, 16.67 Si and 33.33 C theoretical).

If the only impurity occurring with Ti_3SiC_2 is supposed to be TiC, the solid can be considered as consisting of a mixture of 95 mol % Ti_3SiC_2 and 5 mol % TiC.

2.2 Thermal stability

The phase diagram of the Ti–Si–C system was initially determined by Bruckl [14] at 1200 °C with, as main features, the ternary phase Ti_3SiC_2 (T_1) and the solid solution of carbon in Ti_5Si_3 (T_2). Recently, Wakelkamp *et al.* [9] refined some details of the Ti–Si–C phase diagram by determining two cross-sections at 1100 and 1250 °C. They pointed out that the ternary

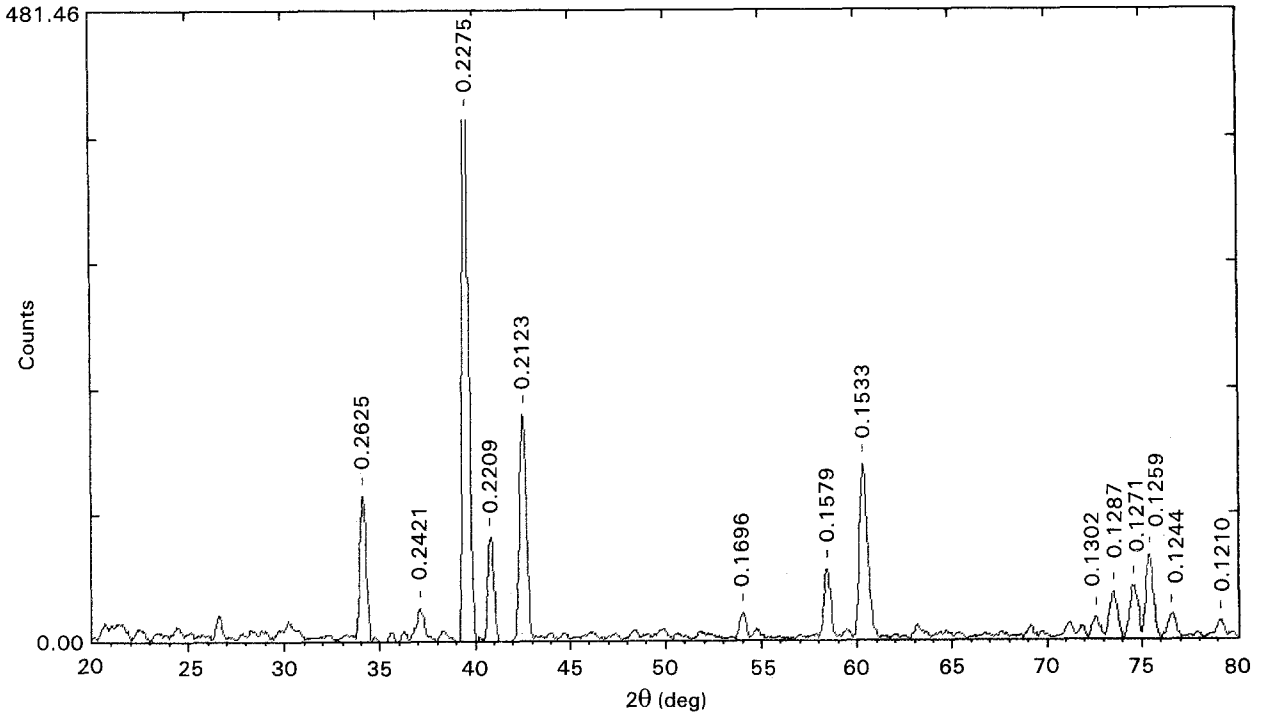

Figure 1 XRD pattern (CuK_α) of Ti_3SiC_2 in the as-prepared state (main impurity: TiC as suggested by the peak at 0.1302 nm).

phase has a small homogeneity range at 1100 °C and becomes a line compound at 1250 °C. Up to now, nothing has been known beyond this temperature. In order to characterize the thermal stability of Ti_3SiC_2 up to 1400–1600 °C, various techniques such as thermogravimetric analysis (TGA), differential thermal analysis (DTA), thermal expansion tests, XRD, EPMA and mass spectrometry were used in present work.

The first experiments were carried out in a graphite crucible under argon (static pressure of 100 kPa). The results of a TGA–DTA experiment are reported in Fig. 2 showing the relative mass variations $\Delta m/m_0$ and its derivative as a function of temperature with a heating rate of 10 °C min^{-1}. A significant mass loss is observed for temperatures higher than 1300 °C. At 1600 °C the mass loss is about 8%. The relative mass variations $\Delta m/m_0$ versus time at 1300 and 1350 °C are shown in Fig. 3. At 1300 °C, a very slight weight loss occurs within the first 30 min and is followed by a constant-weight plateau during the three subsequent hours investigated. After this treatment, the XRD pattern is not changed with respect to the initial one. Conversely, at 1350 °C the relative mass decreases continuously with a constant rate of about 1% per hour. After such a 6 h treatment the resulting solid, analysed by XRD and EPMA, contains titanium carbide but no free or bound silicon. Free silicon is found to occur mixed with the graphite of the crucible. The parameter of the cubic cell of the resulting titanium carbide was refined by using a monocrystalline silicon standard and found to be 0.43214 nm. According to the relationship between the C/Ti ratio in TiC_x and the lattice parameter reported by Storms [15], the solid phase resulting from the decomposition of Ti_3SiC_2 at 1400 °C is mainly $TiC_{0.67}$.

Similar experiments were performed in an alumina crucible. After an isothermal treatment of several hours at 1350 °C, no mass variations were detected and at 1450 °C, a continuous mass loss of about 0.1% per hour was observed during several tens of hours. After 70 h at 1450 °C, the resulting solid consisted of a mixture of Ti_3SiC_2 and titanium carbide.

Recorded under the same conditions as TGA, the corresponding differential scanning calorimetry (DSC) curve exhibits a small exothermic peak between 1450 and 1500 °C, where the mass loss becomes faster. The thermal expansion, also investigated under an Ar atmosphere, is plotted versus temperature in Fig. 4, the heating rate being 10 °C min^{-1}. Up to 900 °C, a classical positive expansion is observed with almost linear variations over a wide temperature range ($\alpha \simeq 0.02 \times 10^{-6}$ °C^{-1} for $100 \leq T \leq 600$ °C and 0.12×10^{-6} for $700 \leq T \leq 900$ °C). Beyond 900 °C, the expansion decreases and even becomes negative for temperatures higher than 1100 °C. This contraction is stopped at about 1400 °C and a high expansion is then observed.

The last experiments for investigating the thermal stability of Ti_3SiC_2 were carried out under vacuum in a graphite crucible. A TGA curve is reported in Fig. 5 with the corresponding thermal programme which includes successive rising temperature steps and constant temperature steps within the range 1100–1400 °C. Up to 1300 °C the mass variations are negligible ($\Delta m/m_0 \leq 0.2\%$), but as soon as the temperature is raised beyond 1300 °C the relative mass decreases rapidly, which confirms the results obtained

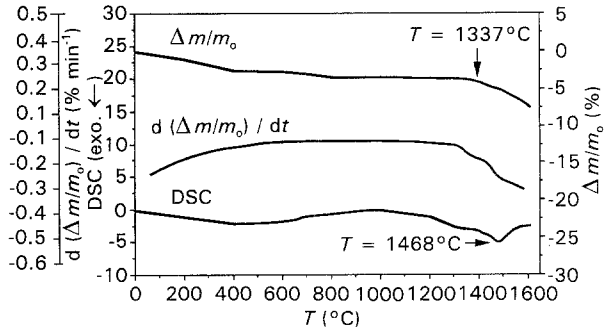

Figure 2 Variation of the relative mass loss ($\Delta m/m_0$), its derivative with respect to time ($d(\Delta m/m_0)/dt$) and DTA signal, recorded during a differential scanning calorimetry (DSC) test on Ti_3SiC_2 run under flowing argon (P = 100 kPa). Heating rate 10 °C min^{-1}.

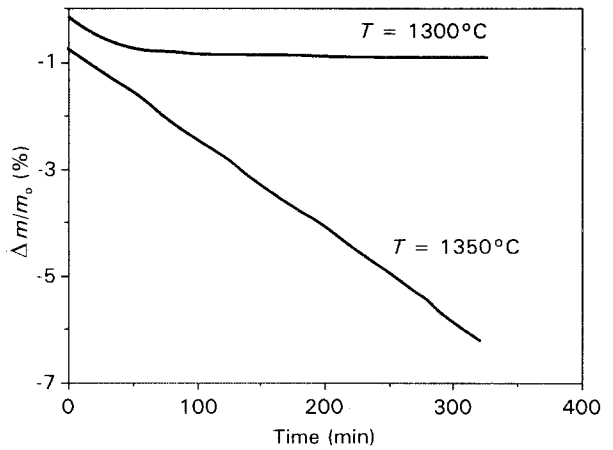

Figure 3 Variations of the relative mass loss $\Delta m/m_0$ as a function of time during a TGA test performed on Ti_3SiC_2 under flowing argon (P = 100 kPa).

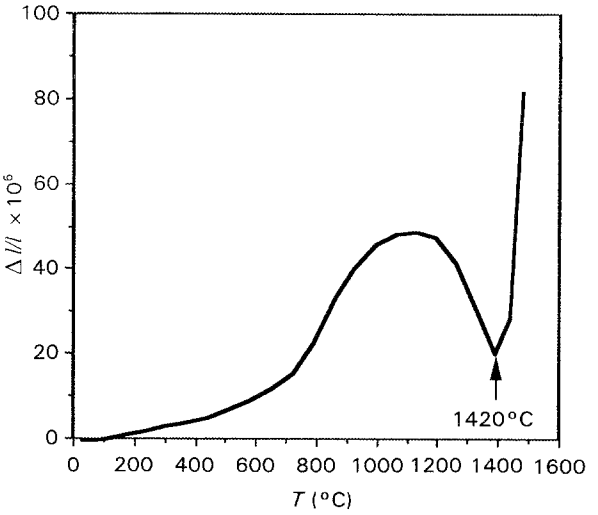

Figure 4 Thermal expansion of Ti_3SiC_2 under an atmosphere of argon within the 25–1500 °C temperature range. Heating rate 10 °C min^{-1}.

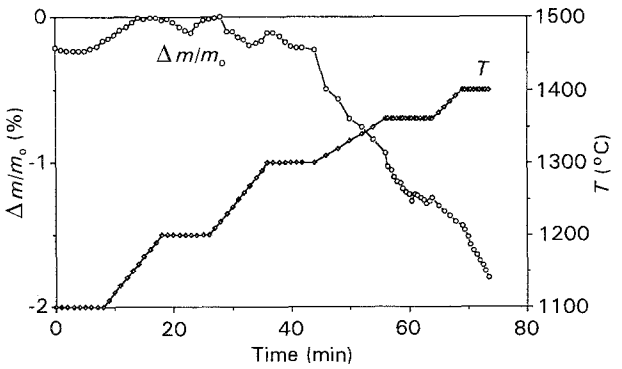

Figure 5 Continuous relative mass change $\Delta m/m_0$ as a function of temperature and time for Ti_3SiC_2 during a test performed under dynamic vacuum.

under an argon pressure of 100 kPa in a graphite crucible. Finally, the ternary phase treated under vacuum at 1400 °C involves the evolution of gaseous silicon, as detected by mass spectrometry.

The presently reported data show that Ti_3SiC_2 is thermally stable up to about 1300 °C. Above this temperature, it undergoes a decomposition and the kinetics is highly dependent on the nature of the medium which surrounds Ti_3SiC_2. A graphite crucible seems to initiate the decomposition process, resulting in a decomposition threshold temperature 150 °C lower than for an alumina crucible, in which Ti_3SiC_2 is stable up to about 1450 °C and then is decomposed very slowly.

The following reaction can be responsible for the decomposition of Ti_3SiC_2:

$$Ti_3SiC_2(s) \rightarrow 3TiC_{0.67}(s) + Si(g)$$
$$\Delta G(1600\ K) = 181\ kJ\,mol^{-1} \quad (2)$$

In the graphite surrounding medium, Reaction 2 can be favoured by SiC formation according to the equation

$$Si(g) + C \rightarrow SiC \quad \Delta G(1600\ K) = -276\ kJ\,mol^{-1} \quad (3)$$

The kinetics of this reaction strongly depends on the morphology of the carbon used. In the present case the graphite of the crucible has a very good crystallization state. Consequently, the reactive carbon sites are only located at the boundaries of the graphitic domains, where Reaction 3 takes place. This reaction can be assumed to initiate the decomposition of Ti_3SiC_2. In addition, when no more reactive sites of carbon occur, the decomposition continues according to Reaction 2 with gaseous silicon evolution which is responsible for the mass loss observed.

In the alumina surrounding medium, reactions between Si(g) and Al_2O_3 are not highly favoured and cannot have any influence on the decomposition of Ti_3SiC_2. Consequently, in the present case, a higher temperature (1450 °C) is required to start the decomposition of Ti_3SiC_2 according to Reaction 2 which exhibits a very slow kinetics.

2.3. Oxidation resistance

Titanium carbide exhibits a rather limited oxidation resistance. A mass increase was observed when TiC was treated under an oxygen pressure between 4 and 16 kPa, at a temperature as low as 350 °C [16]. Titanium oxycarbides and suboxides were assumed to be formed at the beginning of the oxidation process. Non-protecting anatase TiO_2 layers were also reported to form in oxidation tests performed up to 700 °C. If the occurrence of protective rutile TiO_2 films was detected between 700 and 900 °C, a detrimental further oxidation was observed as a result of cracks occurring in the oxide layers when they became rather thick [15, 17]. Owing to the silicon atoms of the ternary phase Ti_3SiC_2, the oxidation behaviour of this compound should be somewhat different from that of TiC and the role played by silicon has to be investigated.

A TGA of Ti_3SiC_2, carried out under 100 kPa of flowing dry oxygen with a heating rate of 10 °C min^{-1}, is shown in Fig. 6. A mass increase starts at about 400 °C and continues up to 1200 °C. Above this temperature the sample mass becomes constant and the total mass gain is of the order of 45%.

The isothermal relative mass variations $\Delta m/m_0$ versus time at temperatures between 450 and 1250 °C under flowing oxygen are shown in Fig. 7. All the isotherms exhibit two steps. The first ($t < 20$–30 min) corresponds to very rapid oxidation kinetics, the mass gain varying from 5 to 45% according to the treatment temperature. The second step is a much slower

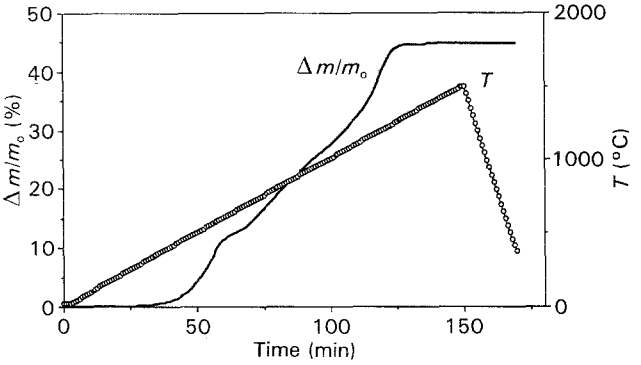

Figure 6 Variations of the relative mass $\Delta m/m_0$ of Ti_3SiC_2 as a function of time and temperature under flowing dry oxygen (P = 100 kPa). Heating rate 10 °C min^{-1}.

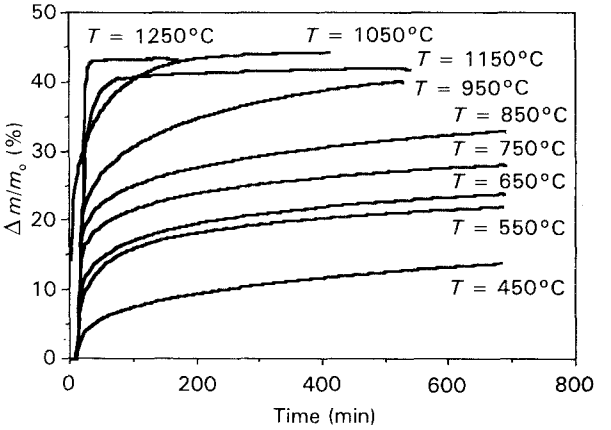

Figure 7 Isothermal weight variations versus time, during the oxidation of Ti_3SiC_2 under flowing dry oxygen (P = 100 kPa) for 450 < T < 1250 °C.

oxidation process with a mass increase of less than 10% for a 10 h treatment. This two-step behaviour is enhanced at high temperature, i.e. for $T \geq 1150\,^{\circ}C$. It is worthy of note that in the second regime, the mass gain is lower at 1150 °C than at 1050 °C.

The samples resulting from an oxidation of 6 h under flowing oxygen, i.e. within the second oxidation regime, were characterized from a physico-chemical point of view: identification of the various phases by XRD, morphology by SEM and distribution of the phases within the oxidized grains by Auger electron spectroscopy (AES) depth profiling.

Fig. 8 shows the XRD patterns of the samples oxidized at 650, 950 and 1150 °C. At 650 °C three phases are identified: both modifications of TiO_2 (i.e. anatase and rutile), and Ti_3SiC_2 which has been only partially oxidized (Fig. 8a). At 950 °C the extent of oxidation is higher, as evinced by a decrease of the Ti_3SiC_2 lines, and the only oxide phase is rutile (Fig. 8b). At 1150 °C Ti_3SiC_2 peaks do not appear any longer in the pattern, which means that the ternary phase is almost totally oxidized, giving rise to rutile-type TiO_2 and cristobalite SiO_2 (Fig. 8c).

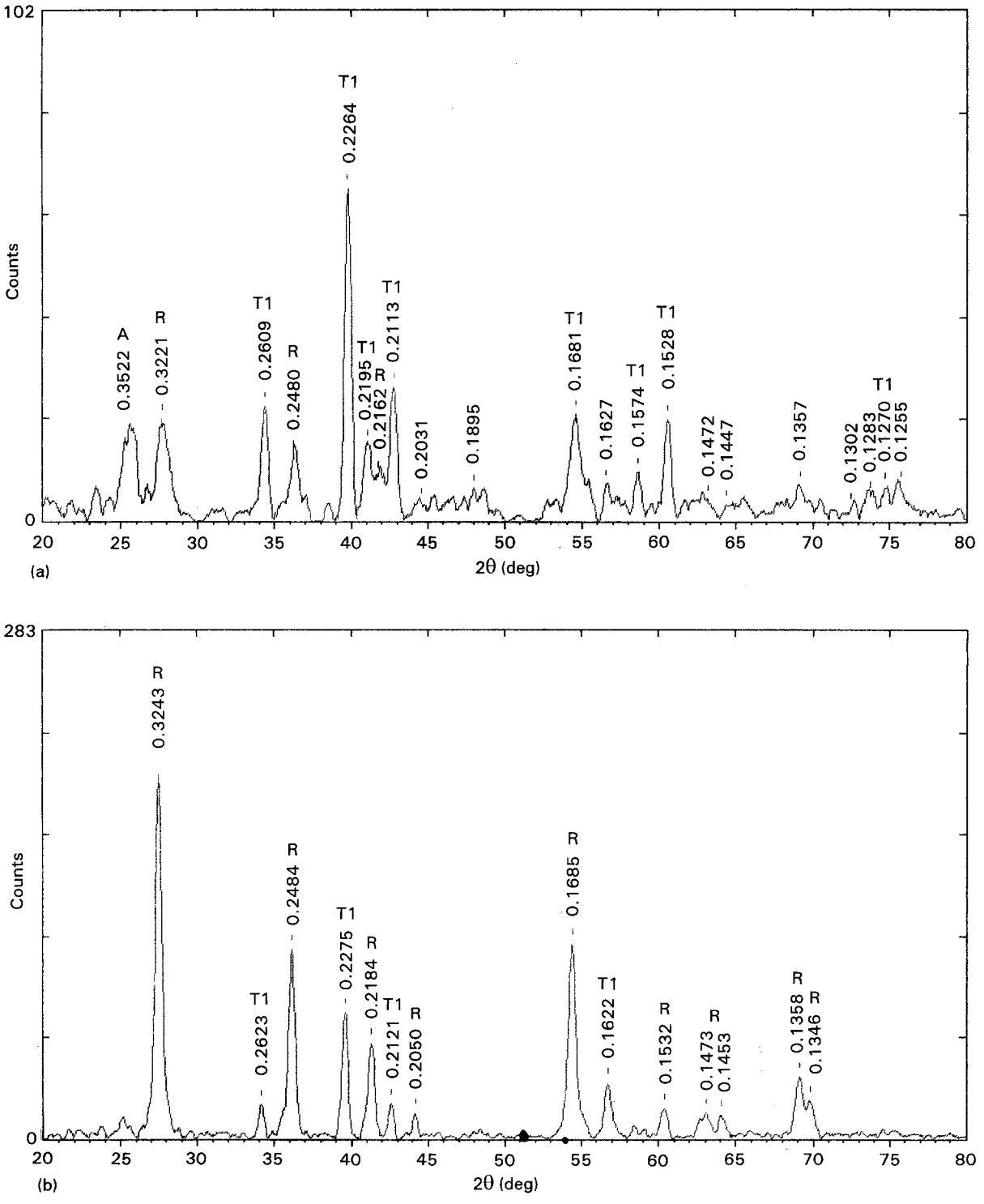

Figure 8 XRD patterns (CuK_α) of the solid residue after an oxidation treatment of Ti_3SiC_2 in flowing oxygen (P = 100 kPa) at (a) 650 °C, (b) 950 °C and (c) 1150 °C. T1 = Ti_3SiC_2, A = TiO_2 anatase, R = TiO_2 rutile, S = SiO_2 cristobalite.

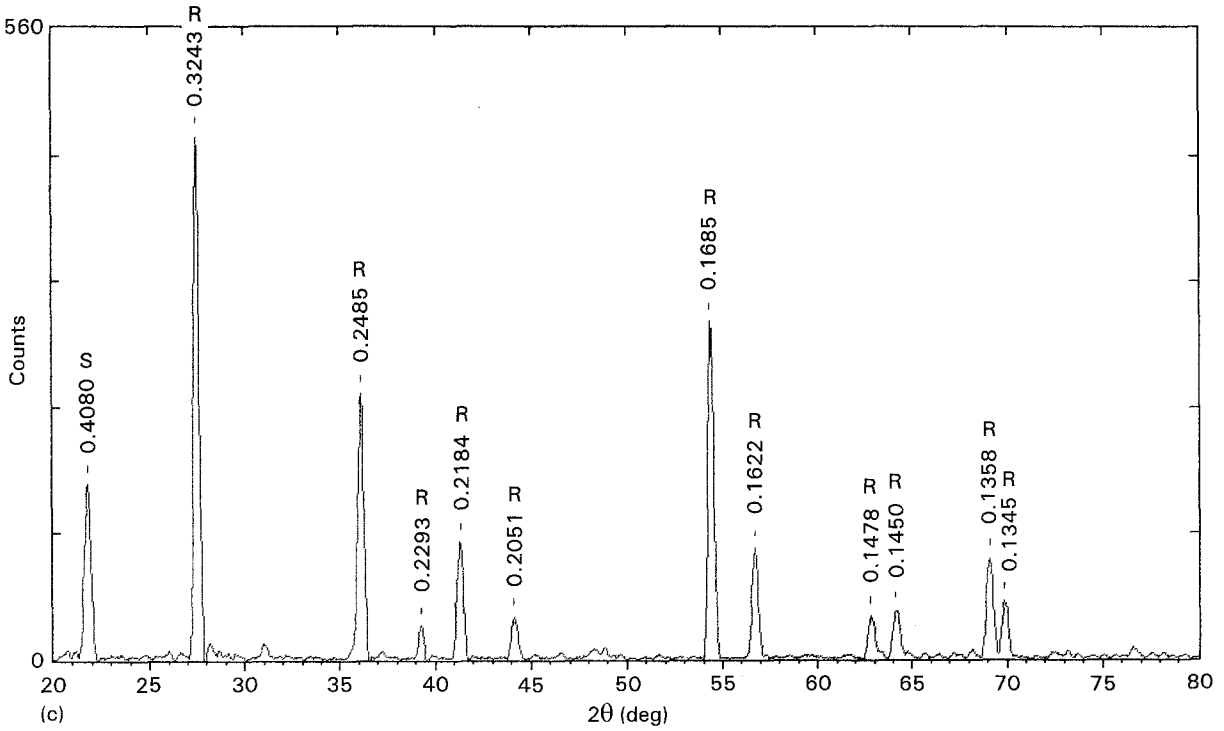

Figure 8 (Contd.)

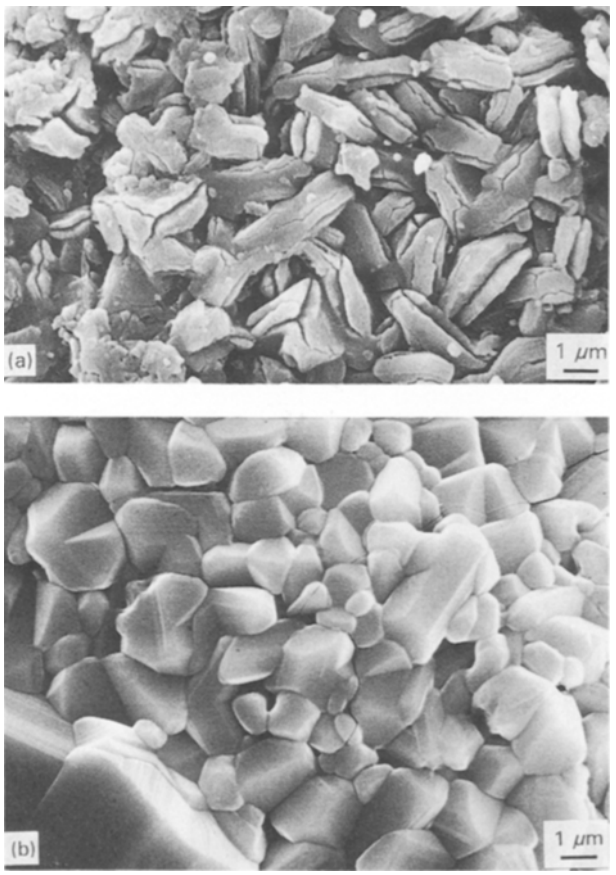

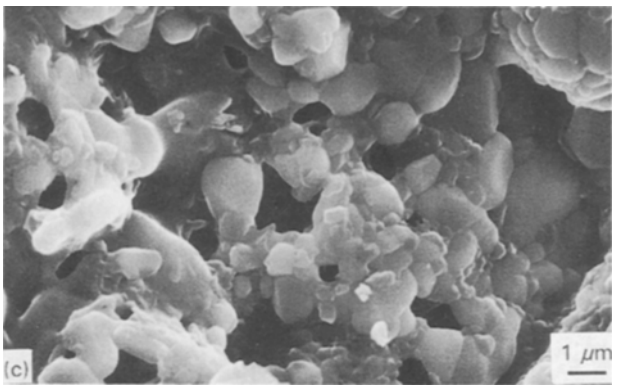

Figure 9 SEM images of the solid residue obtained after an oxidation treatment of Ti_3SiC_2 in flowing oxygen (P = 100 kPa) at (a) 650 °C, (b) 950 °C and (c) 1150 °C.

The morphology of the Ti_3SiC_2 samples after the various previously defined oxidation treatments was observed by SEM (Fig. 9). At 650 °C the sample grains are cracked particularly along the edges (Fig. 9a). These cracks are very similar to those reported by Shimada and Kozeki [16] for the oxidation of titanium carbide at only 400 °C. These authors assigned these cracks to the stress developed within the anatase layer and resulting from the volume expansion associated with the oxidation of TiC into anatase. At 950 °C no cracks are present any longer and the grains are joined together (Fig. 9b). At 1150 °C the original individual grains are no longer present and pores occur within a solid which seems to have been partially melted (Fig. 9c).

AES depth profiling, i.e. atomic concentration–sputtering time curves, were recorded by sputtering samples oxidized at 650 and 1150 °C, as shown in Fig. 10. For the oxidation at 650 °C, the analysis suggests the occurrence of (i) titanium oxide coating the Ti_3SiC_2 phase and (ii) a mixture of titanium oxide with small amounts of SiO_2 as external layer (Fig. 10a). For the oxidation at 1150 °C a mixture of

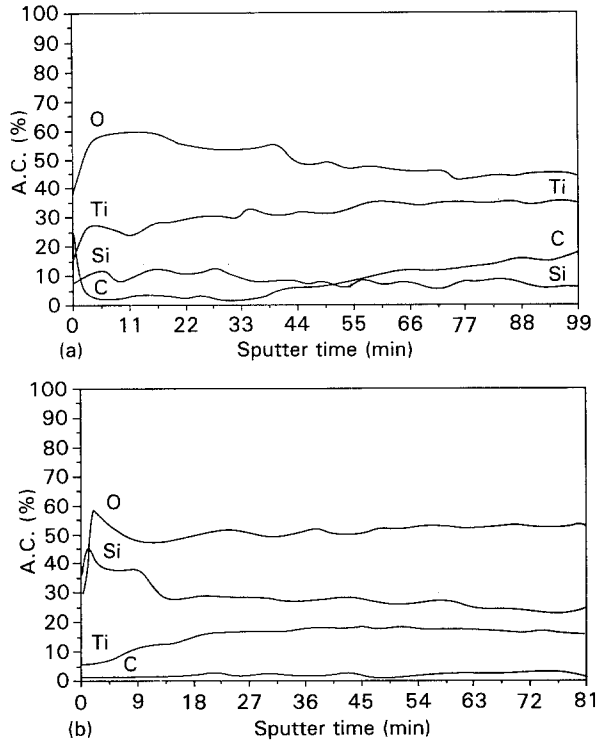

Figure 10 AES depth-profiles (A.C. = atomic concentration) recorded for Ti_3SiC_2 samples after an oxidation treatment under flowing oxygen (P = 100 kPa) at (a) 650 °C and (b) 1150 °C (sputter rate 50 nm min^{-1}, standard Ta_2O_5).

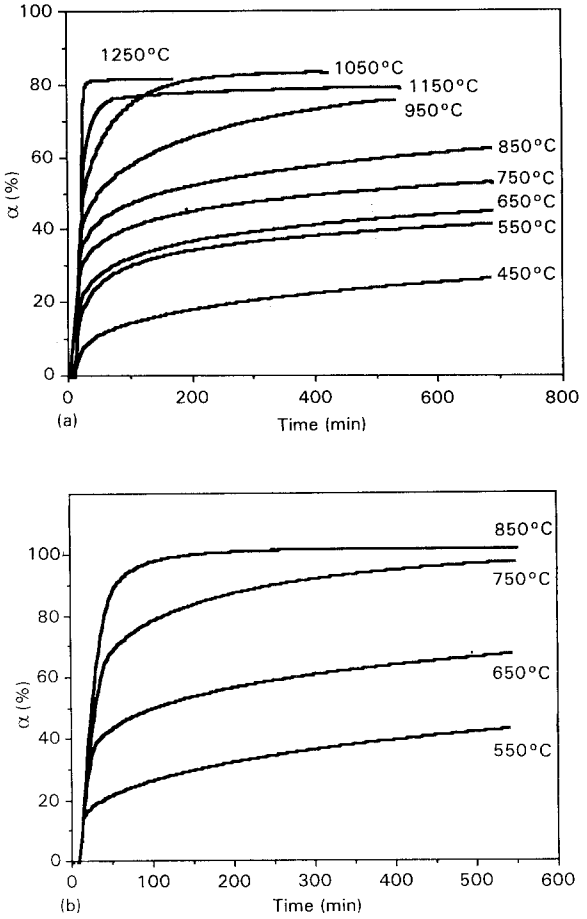

Figure 11 Percentage of oxidized (a) Ti_3SiC_2 and (b) TiC versus time (a) between 450 and 1250 °C and (b) between 550 and 850 °C, during oxidation under flowing dry oxygen (P = 100 kPa).

titania and silica is evinced, coated with a thin layer enriched in SiO_2 (Fig. 10b).

On the basis of these investigations, the oxidation behaviour of Ti_3SiC_2 can be deduced. The oxidation starts at 400 °C (Fig. 6), which is slightly higher than for TiC. Three temperatures domains can be described separately, but without drastic behaviour changes between them.

In the first temperature range, i.e. 650–850 °C, the oxidation process results in the formation of both anatase and rutile. At the beginning of the oxidation, a TiO_2 film is rapidly formed by direct reaction of oxygen with Ti_3SiC_2, which corresponds to the first step reported in Fig. 7. This TiO_2 film becomes rapidly protecting, giving rise to the second step related to a slow formation of TiO_2 and SiO_2 by diffusion of (i) oxygen atoms towards the core of the sample and (ii) silicon atoms towards the external surface. Owing to the stoichiometry of the ternary phase, the amount of SiO_2 is low with respect to that of TiO_2. The silica component of the oxidation product formed in the 650–850 °C temperature range is probably amorphous. Its occurrence was shown by XRD after a 1200 °C treatment under an Ar atmosphere followed by a slow cooling, resulting in SiO_2 crystallization. As the oxidation is going on the growth of the oxide layer gives rise to cracks in this layer, owing to the volumic expansion (of about 100%) related to TiO_2 and SiO_2 formation from Ti_3SiC_2 (Fig. 9a).

The main reaction involved in the oxidation process corresponds to the overall equation

$$Ti_3SiC_2 + 6O_2 \rightarrow 3TiO_2 + SiO_2 + 2CO_2 \quad (4)$$

The corresponding theoretical mass gain is 53% under the assumption of a complete reaction. This percentage is rather close to the experimental mass gain of 45% observed at the end of the oxidation. On this basis, the fraction reacted α can be calculated by dividing the measured mass increase by the theoretical one. If the same definition is used for the oxidation of titanium carbide with respect to the equation

$$TiC + 2O_2 \rightarrow TiO_2 + CO_2 \quad (5)$$

a comparison is possible between Ti_3SiC_2 and TiC oxidation behaviours (Fig. 11). A quasi-complete oxidation of TiC is achieved after about 1 h treatment at 850 °C while it needs about 3 h at 1050 °C for Ti_3SiC_2. Two reasons can be given for this Ti_3SiC_2 oxidation process being slower than that of TiC: (i) a more difficult diffusion of oxygen within stoichiometric SiO_2 than within a defective TiO_2 structure (oxygen vacancies or insterstitial titanium ions), and (ii) cracks occurring in the oxide layers of both materials which may be partially filled by amorphous SiO_2 only for Ti_3SiC_2. In both explanations the protecting effect of SiO_2 is involved. The present comparison can be refined by investigating more precisely both kinetic regimes. The beginning of the oxidation at 850 °C is shown in Fig. 12. For Ti_3SiC_2, a transition from a rapid kinetic regime to a slow one occurs after less than 20 min. Conversely, no transition is observed in

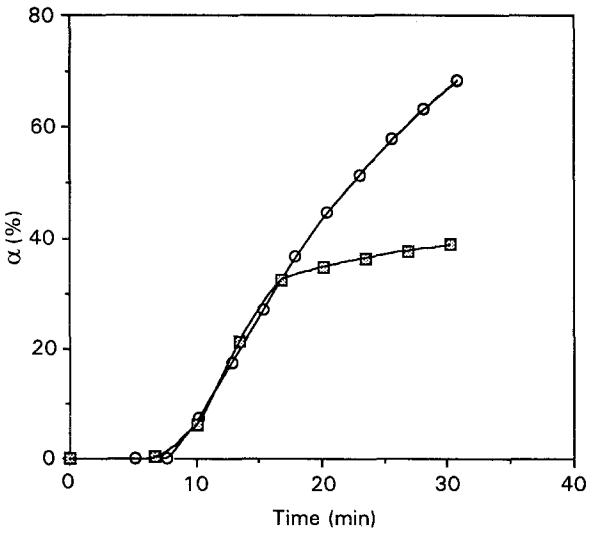

Figure 12 Variations of the percentage α of (○) TiC or (□) Ti_3SiC_2 oxidized as a function of time during an oxidation test in flowing oxygen at 850 °C.

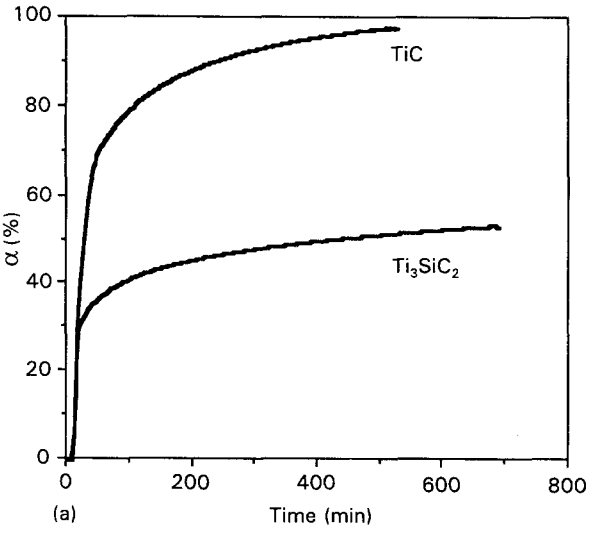

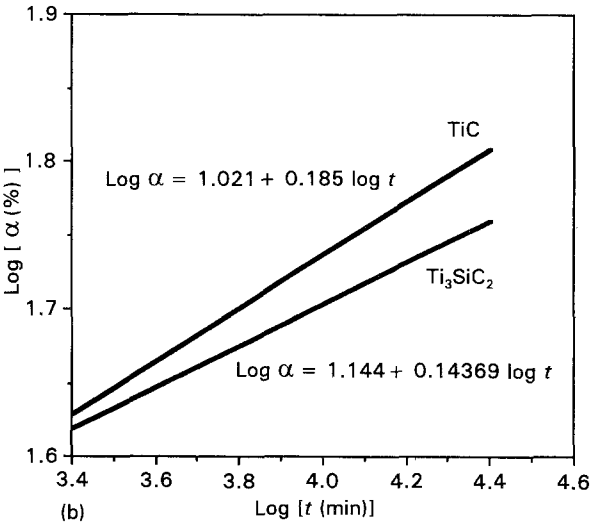

Figure 13 (a) Variations of the percentage of TiC or Ti_3SiC_2 oxidized as a function of time t during an oxidation test at 750 °C in flowing oxygen (P = 100 kPa) and (b) the same data in log–log coordinates.

the same range of treatment duration for TiC which is continuously oxidized with a relatively high rate. The comparison between the Ti_3SiC_2 and TiC oxidation kinetics is clearly shown for T = 750 °C in Fig. 13. A slow regime occurs for Ti_3SiC_2 with an oxidation extent limited to 50% after 10 h, while that of TiC reaches almost 100% which corresponds to a more rapid oxidation rate (Fig. 13a). If the oxidation extent α is drawn as a function of time in log–log coordinates, the oxidation behaviour law can be written between 30 and 600 min as

$$\alpha^n = kt \qquad (6)$$

where $n \simeq 5$ for TiC and $n \simeq 7$ for Ti_3SiC_2 (Fig. 13b). These results confirm the role played by silicon atoms in the oxidation of the ternary phase Ti_3SiC_2, i.e. the protecting effect of silica formed during the oxidation process.

In a second temperature range, i.e. 850–1050 °C, the process of oxidation of Ti_3SiC_2 is more rapid. Thermal activation occurs in both kinetic regimes, i.e. that controlled by a direct oxidation reaction at the beginning of the process (during about 20 min) and that governed by diffusion through the oxide layers. The oxides are mainly TiO_2 (rutile) and to lesser extent amorphous SiO_2 which occurs particularly near the surface of the grains. This SiO_2 film probably joins the grains together, contributing to prevent a rapid oxidation (Fig. 9b). After a 10 h treatment the oxidation extent is about 70% (Fig. 11).

In the third temperature range, i.e. 1050–1250 °C, the oxidation rate reaches its maximum with an extent of 80%. A mixture of TiO_2 (rutile) and SiO_2 occurs in the bulk and is coated by a thin layer of SiO_2. Under these conditions, SiO_2 crystallizes as cristobalite (Fig. 8c). This maximum oxidation extent of 80% shows that either a small amount of Ti_3SiC_2 is totally protected against oxygen or Equation 4 does not represent exactly the oxidation process. Both explanations can be simultaneously referred to. Finally, the mass gain found lower at 1150 than 1050 °C (Fig. 7) can result from (i) the evolution of a small amount of SiO and/or (ii) the lowering of the oxidation kinetics by inhibition of oxygen diffusion through crystallized SiO_2 with respect to amorphous SiO_2 [18].

Acknowledgements

The authors wish to thank Dr F. Lamouroux for helpful discussions in the field of oxidation processes and M. Lahaye and L. Rabardel for their contribution to the AES and thermal analyses, respectively. They are indebted to Société Européenne de Propulsion and CNRS for their support via a grant to C. Racault.

References

1. W. JEITSCHKO and H. NOWOTNY, *Mh. für Chem.* **98** (1967) 329.
2. P. MARTINEAU, R. PAILLER, M. LAHAYE and R. NASLAIN, *J. Mater. Sci.* **19** (1984) 2749.
3. S. MOROZUMI, M. ENDO, M. KIKUCHI and K. HAMAJIMA, *ibid.* **20** (1985) 3976.
4. T. ISEKI, T. YANO and Y. S. CHUNG, *J. Ceram. Soc. Jpn. Int. Ed.* **97** (1989) 697.

5. M. BACKHAUS-RICOULT, *Ber. Bunsenges. Phys. Chem.* **93** (1989) 1277.
6. S. K. CHOI, M. CHANDRASEKAN, and M. J. BRABERS, *J. Mater. Sci.* **25** (1990) 1957.
7. B. GOTTSELIG, E. GYARMATI, A. NAOUMIDIS and H. NICKEL, *J. Eur. Ceram. Soc.* **6** (1990) 153.
8. T. NISHINO, S. URAI and M. NAKA, *Eng. Fract. Mech.* **40** (1991) 829.
9. W. J. J. WAKELKAMP, F. J. J. van LOO and R. METSELAAR, *J. Eur. Ceram. Soc.* **8** (1991) 135.
10. J. J. NICKL, K. K. SCHWEITZER and P. LUXENBERG, *J. Less-Common Met.* **26** (1972) 335.
11. T. GOTO and T. HIRAI, *Mater. Res. Bull.* **22** (1987) 1195.
12. R. PAMPUCH, J. LIS, L. STOBIERSKI and M. TYMKIEWICZ, *J. Eur. Ceram. Soc.* **5** (1989) 283.
13. S. SAMBASIVAN, PhD Dissertation, Arizona State University, Tempe, AZ (1990).
14. C. E. BRUCKL, "Ternary phase equilibria in transition boron–carbon–silicon systems", Part II, Vol. VII, AFML-TR-65-2 (Metals and Ceramic Division, Air Force Laboratory, Wright Patterson Air Force Base, Ohio, 1966).
15. E. K. STORMS, "The Refractory Carbides" (Academic, New York, 1967) p. 1.
16. S. SHIMADA and M. KOZEKI, *J. Mater. Sci.* **27** (1992) 1869.
17. Y. A. LAVRENKO, L. A. GLEBOV, A. P. POMITKIN, V. G. CHUPRINA and T. G. PROTSENKO, *Oxid. Met.* **9** (1975) 171.
18. T. NARUSHIMA, T. GOTO and T. HIRAI, *J. Amer. Ceram. Soc.* **72** (1989) 1386.

Received 3 December 1993
and accepted 19 January 1994